LIGHTNING OVERVOLTAGES IN POWER SYSTEMS

Juan A. Martinez-Velasco
Universitat Politècnica de Catalunya, Barcelona, Spain

Ferley Castro-Aranda
Universidad del Valle, Cali, Colombia

Keywords: Lightning flash, lightning stroke, lightning overvoltage, ground flash density, keraunic level, incidence model, electrogeometric model, flashover, flashover rate, backflashover, backflashover rate, lightning induced overvoltage, lightning induced flashover rate, shielding failure, shielding failure flashover rate, shield wire, footing impedance, corona, modeling, Monte Carlo analysis.

Contents

Summary

Lightning is one of the main causes of overvoltages in power systems. Assessing lightning overvoltages is crucial for designing lines and substations, and for their protection. Lightning overvoltages are fast-front transient voltages mainly caused by the impact of lightning return strokes to overhead lines. Therefore, it is very important analyzing the lightning performance of an overhead line and the methods that can be implemented for improving their performance (e.g., by shielding the line with shield wires installed at the top of towers or poles).

Direct strokes to substations are generally ignored, since it is assumed that only lightning return strokes with a peak current magnitude below the critical value will hit substation equipment. This chapter is basically aimed at analyzing the lightning performance of overhead transmission and distribution lines; that is, the chapter provides the methods for determining the flashover rate of overhead lines, assuming by default that transmission lines are shielded and distribution lines are not shielded. Therefore, a flashover in an overhead line can be caused, depending on the line design and its voltage level, by either a direct stoke to a phase conductor, a direct stroke to a shield grounded wire, or a nearby stroke to ground (i.e., flashover caused by induced overvoltages).

Lightning is random in nature, so the statistical variations of the lightning-stroke parameters must be taken into account. Important aspects for evaluating the lightning performance of power overhead lines are an accurate knowledge of lightning strokes parameters and the application of an incidence model, used to estimate the number of direct return strokes to a line or to the vicinity of the line. The chapter details the mechanism of lightning discharges and their characterization, summarizes some of the procedures developed for estimating the lightning performance of overhead lines, presents the guidelines proposed for representing overhead lines in lightning

overvoltage studies, and includes some illustrative test cases aimed at determining the lightning performance of transmission and distribution overhead lines.

1. Introduction

Lightning discharges are one of the primary causes of failure of high voltage power equipment. Lightning studies are performed to design lines and substations, and for the protection of power system equipment (Hileman, 1999; Chowdhuri, 1996; Greenwood, 1991; Anderson, 1982). Some of the objectives of these studies are to characterize the lightning overvoltages for insulation requirements, and to find the critical lightning stroke current that causes insulation flashover. Specific objectives for overhead lines may be to determine lightning flashover rate (LFOR) and select line arresters. For substations the objectives may be to calculate Mean Time Between Failure (MTBF), determine surge arrester ratings, find optimum location of surge arresters for lightning surge protection, or estimate minimum phase-to-ground and phase-to-phase clearances (Hileman, 1999).

Lightning overvoltages are fast-front transient voltages mainly caused by the impact of lightning return strokes to overhead lines. The lightning performance of an overhead line can be improved by shielding the line with shield wires installed at the top of towers or poles. Shield wires are aimed at preventing the impact of return strokes to active phase conductors. Most transmission lines are shielded, so lightning overvoltages in these lines are caused by return strokes to a phase conductor, to a tower or to a shield wire. Most distribution lines are not shielded, so lightning flashovers may be caused by direct strokes to the line conductors or induced by strokes to ground in the vicinity of the line.

Direct strokes to phase conductors: Direct strokes to the phase conductors of a shielded line occur typically when lightning strokes of low magnitude (a few kA) bypass the shield wires (*shielding failure*). Traditionally, the electrogeometric model based upon a strike distance has been used to determine the maximum prospective peak current magnitude that can bypass the shielding and hit on phase conductors. A detailed description of this model can be found in the literature (Hileman, 1999). A usual approach has been to design the line insulation to withstand the maximum shielding failure current predicted by the electrogeometric model without an outage to the line.

Direct strokes to shield wires: When the lightning discharge strikes the tower or the shield wire, the resultant tower top voltage may be large enough to cause flashover of the line insulation from the tower to the phase conductor. This event, known as *backflashover*, is of great concern. When backflashover occurs, a part of the surge current will be transferred to the phase conductors through the arc across the insulator strings. By default, it is assumed that the backflashover causes a temporary phase-to-ground fault that will be cleared by a circuit breaker. A line outage results until the circuit breaker is reclosed. The voltage surge as a result of the backflashover is very steep. The steepness and the magnitude of the voltage decrease as the surge propagates along the line, depending upon the line parameters. Corona is another important factor that reduces the steepness of the incoming voltage surge.

Direct strokes to substations are generally ignored, since it is commonly assumed that the substation is perfectly shielded, via shield wires or lightning masts; that is, only strokes with a peak current magnitude below the critical value will hit substation equipment. For substation design studies, lightning is assumed to hit a nearby tower or shield wire of an incoming line causing a backflashover. The resultant lightning surge enters the substation and propagates inside. A discontinuity exists at junction points where a change in height or cross section of the busbar takes place, and at equipment terminals. The discontinuity points inside the substation, status of circuit breakers/switches (open/close), and location of lightning arresters are especially important for the overvoltage characterization at the substation. These overvoltages will provide the data required for insulation coordination and arrester specifications.

This chapter is basically aimed at analyzing the lightning performance of overhead transmission and distribution lines; that is, the chapter provides the methods for determining the flashover rate of overhead lines, assuming by default that transmission lines are shielded and distribution lines are not shielded.

An important aspect for these studies is the characterization of lightning. An accurate knowledge of the parameters of lightning strokes is essential for predicting the severity of the transient voltages generated by lightning discharges. However, lightning is random in nature; no two lightning strokes are the same. Therefore, the statistical variations of the lightning-stroke parameters must be taken into account and they must be expressed in probabilistic terms from data measured in the field (CIGRE WG 33.01, 1991; IEEE TF, 2005). The next two sections detail the mechanism of lightning discharges and their characterization. Another important aspect for assessing the lightning performance of overhead lines is the application of an incidence model that can estimate the number of direct return strokes to a line or to the vicinity of the line. This is the main goal of Section 4, in which the electrogeometric model is presented and applied.

The approaches that can be considered for representing an overhead line in lightning studies are presented in Section 5. Although this section is basically dedicated to modeling transmission lines, many of the concepts can be also useful for distribution lines. The next two sections, namely Sections 6 and 7, introduce procedures for estimating the lightning performance of transmission and distribution lines. The procedures are based on those recommended by CIGRE WG 33.01 (1991) IEEE Std. 1243 (1997), and IEEE Std 1410 (2010).

2. The Mechanism of Lightning

2.1. Cloud Charges and Lightning Discharges

Most clouds consist of liquid droplets and form at altitudes of more than 1 km from earth's surface, where temperatures are above freezing. Figure 1 shows the three charge regions that have been confirmed by measurements. Below region A, the vertical movement of the raindrops and the wind shear splits the raindrops into negatively charged small drops and positively charged larger raindrops; raindrops do not fall through in this region. The velocity of air currents in region A is high enough to break

falling raindrops, causing positive charge spray in the cloud and negative charges in the air. The spray is blown upward, but as the velocity decreases, the positively charged drops combine with larger drops and fall again. Region A becomes positively charged, while region B becomes negatively charged due to air currents. In the upper regions, the temperature is below the freezing point and only ice crystals exist. The main negative charge in the central portion is in the temperature zone between –10ºC and –20ºC. The upper and lower regions in the cloud are separated by a quasi-neutral zone. The positive charge is typically smaller in magnitude than the main negative charge. As the freezing of droplets progresses from outside to inside, the outer negatively charged shells fall off, and the remaining positively charged fragments are moved upward in the convection current. The raindrops have a size of a few millimeters and are polarized by the electric field that is present between the lower part of the ionosphere and the earth's surface. The strength of this atmospheric field is on summer days in the order of 60 V/m and can reach values of 500 V/m on a dry winter day. For more details on this topic see Chowdhuri (1996), van der Sluis (2001), Das (2010), and Rakov & Uman (2006).

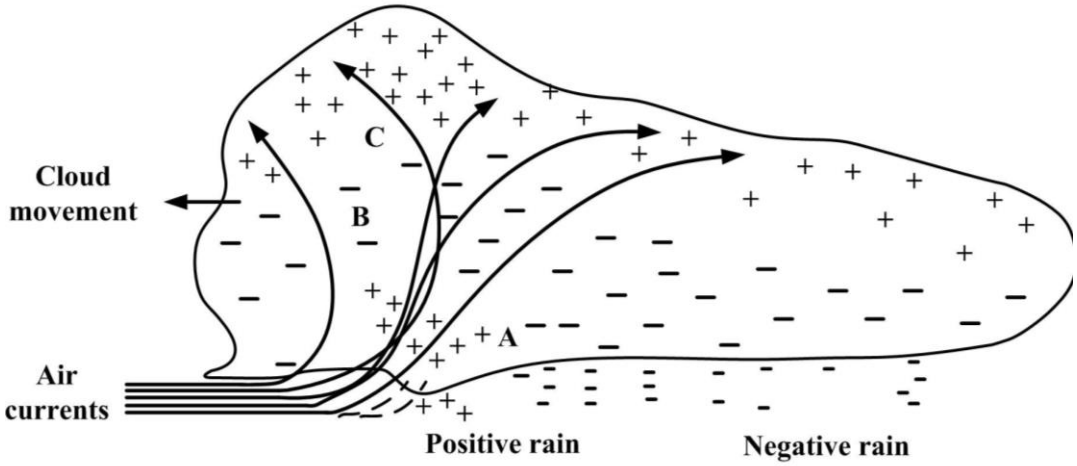

Figure 1. The classic charge structure of a thundercloud.

The majority of the thunderclouds is *negatively* charged with a potential to ground of several hundreds of MegaVolts (MV). The clouds move at great heights and the average field strength is far below the average breakdown strength of air. The wind in the atmosphere create a charging mechanism that separates electric charges, leaving negative charge at the bottom and positive charge at the top of the cloud. As charge at the bottom of the cloud keeps growing, the potential difference between cloud and ground, which is positively charged, grows as well. This process will continue until air breakdown occurs. Inside the thundercloud, the space charge formed by the accumulating negative raindrops creates a local electric field of about 10 kV/m and accelerates the negative ions to considerable velocities. Collision between the accelerated negative ions and air molecules, creates new negative ions, which are accelerated, collide with air molecules and free new negative ions. An avalanche takes place, and both the space charge and the resulting electric field grow in a very short period of time.

The main lightning discharge types are of the following type (see Figure 2) (Hileman, 1999; Das, 2010):

- *Intercloud flash*. It is the most common lightning discharge type, and takes place between upper positive and main negative charge regions of the cloud.
- *Cloud to ground flash*. It generally transfers negative charge from the negative region of the cloud to ground.
- *Air discharge*. It is a discharge in the air that does not touch the ground.

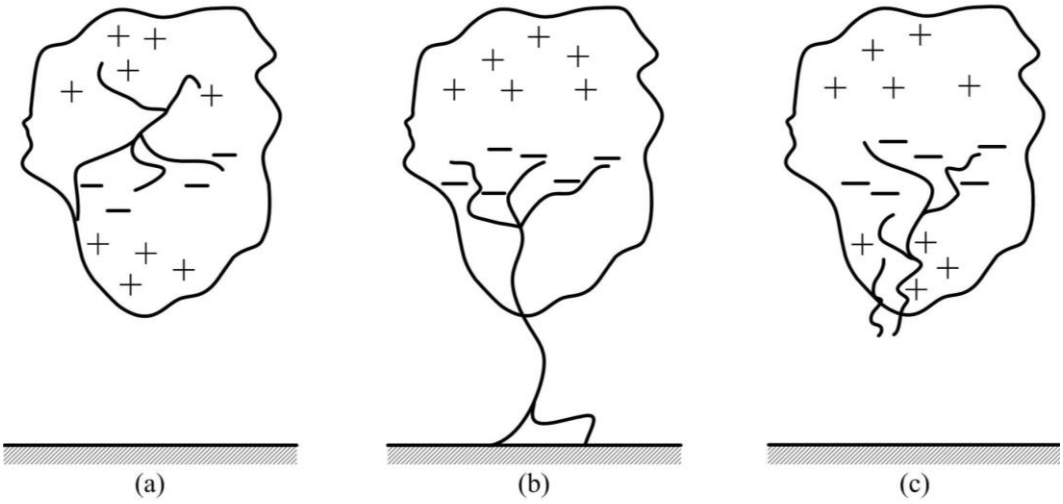

Figure 2. Predominant lightning discharge types: (a) intercloud flash; (b) cloud to ground flash; (c) air discharge.

2.2. The Ground Flash

The ground flash is initiated by electrical breakdown in the cloud, which creates a column of charge called *stepped leader*, which starts traveling downward in a stepped manner. On its way to ground, stepped leaders follow a rather tortuous path, being their propagation random. The stepped leader travels downward in steps several tens of meters in length and pulse currents of at least 1 kA in amplitude. When this leader is near ground, the potential to ground can reach values as large as 100 MV before the attachment process with one of the upward streamers is completed.

The electrical field at ground level increases as the leader approaches the ground. Tall objects, such as trees, power lines, structures, and buildings, are more vulnerable. Around an induced electrical field level of about 3 MV/m, a corona streamer of opposite polarity rises from the object to meet the downward leader. These discharges from the grounded structures, called *connecting leaders*, travel toward the stepped leader. One of the connecting leaders may successfully bridge the gap between the ground and the stepped leader.

This completes the current path between the cloud and the ground, and high discharge current flows to neutralize the charge, positive from ground to negative in the cloud. This is called the *return stroke*, whose velocity is around one-third the speed of light.

The median peak current value associated to the return stroke is reported to be of the order of 30 kA, with rise time and time to half values around 5 and 75 μs, respectively. The creation of the return stroke takes place between 5 and 10 μs. In most cases, the return stroke prevents any further propagation of the leader, as the current path is neutralized. However, two branches of the leader can reach the ground simultaneously, resulting in two return strokes. An upward moving stroke may encounter a branch end and there is an immediate luminosity of the channel; such events are called branch components. In certain cases, the return stroke current may not go to zero quickly and continue to flow for tens to a few hundreds of milliseconds.

The separation between the object struck and the tip of the downward leader is called the *striking distance*, which is of importance in shielding and lightning protection. It is actually under this principle that lightning protection works; see Section 4.

The lightning flash may not end in the first stroke. The depletion of charge in the original cloud cluster creates cloud to cloud discharges and connects the adjacent charge clusters to the original charge cluster, which may get sufficiently charged to create subsequent strokes. Because the discharge path from the original stroke is still ionized, it takes less charge to start a flash. The pre-ionized channel results in subsequent strokes with about one-third the current and shorter rise time in comparison with the original stroke. Sometimes discharges originate several kilometers away from the end of the return stroke channel and travel toward it. These may die out before reaching the end of the return stroke point, but if these discharges make contact with the return-stroke channel and the channel is carrying continuous current, it will result in a discharge that travels toward the ground. If the return stroke channel is in partially conducting stage, it may initiate a dart leader that travels toward the ground. Where ionization has decayed, it will prevent continuous propagation of the dart leader, and it may start propagating to ground as a stepped leader, called *dart-stepped leader*. If these leaders are successful in traveling all the way to ground, then subsequent return strokes occur. It is not uncommon for the leader to take a different path than the first stroke. A ground flash may last up to 0.5 s with a mean number of strokes ranging from 4 to 5. The separation between subsequent channels was observed to be a few kilometers on average. The positive leaders propagate approximately in a similar manner as negative strokes. For more details on this topic see Chowdhuri (1996), van der Sluis (2001), Das (2010), and Rakov & Uman (2006).

Generally, dart leaders develop no branching, and travel downward at velocities of around 3×10^6 m/s. Subsequent return strokes have peak currents usually smaller than first strokes but faster zero-to-peak rise times. The mean inter-stroke interval is about 60 ms, although intervals as large as a few tenths of a second can be involved when a so-called continuing current flows between strokes (this happens in 25–50% of all cloud-to-ground flashes). This current, which is of the order of 100 A, is associated to charges of around 10 C and constitutes a direct transfer of charge from cloud to ground (Rakov & Uman, 2006).

To summarize, a lightning stroke will usually consist of several discharges, usually three or four, with an interval time of 10–100 μs. After each discharge, the plasma channel cools down, leaving enough ionization to create a new conducting plasma

channel for the following discharge. Around half of all lightning discharges to ground, both single- and multiple-stroke flashes, may strike ground at more than one point, with mean separation between channel terminations on ground of 1.3 km.

3. Lightning Characterization

3.1. Introduction

The lightning flash can be firstly categorized by the polarity of the charge (positive, negative) and the direction of propagation (downward, upward). In addition, the lightning flash may contain several strokes (i.e., the first return stroke may be followed by one or more subsequent strokes), so it can be also categorized as single- or multi-stroke.

Upward flashes do usually occur from very tall structures. Since the height of a majority of overhead lines is below 100 m, they are generally subject to downward flashes (CIGRE WG 33.01, 1991). Except for seasonal and regional variations, more than 90% of downward flashes are of negative polarity, with about one half comprising only one stroke.

Multiple-stroke negative flashes comprise three strokes as average, and less than 5% have more than 10 strokes. Based on a survey of almost 6000 flash records from different regions of the world, Anderson and Eriksson estimated the percentages of multiple strokes in negative ground flash shown in Table 1 (IEEE TF, 2005). However, the percentage of single-stroke flashes shown in the table is considerably higher than the figures obtained from some field measurements (de la Rosa, (2007). More than 90% of positive flashes are single-stroke.

Lightning protection systems must be therefore designed to withstand the effect of a series of strokes to the same location within a short period of time.

Number of strokes per flash	Frequency of occurrence (%)
1	45
2	14
3	9
4	8
5	8
6	4
7	3
8	3
9	2
10 or more	4

Table 1. Statistical distribution of multistroke negative lightning flashes

3.2. Lightning Current Waveshape

Lightning stroke currents differ in shape and amplitude. The majority of the cloud-to-ground lightning strokes vary from a few kA to several tenths of kA. Strokes with peak current magnitudes above 100 kA are rare, although peak currents above 200 kA have been reported. The shape of the current wave is variable and different for every stroke. To facilitate testing in the laboratory, the shape of the current wave of the return stroke has been standardized, and the so-called 1.2/50-μs waveshape, see Figure 3, has been adopted (IEC 60071-1, 2010; IEEE Std 1313.1, 1996). The rise time, $t_f = 1.2\ \mu s$, is defined as being 1.67 times the time interval between 30% and 90% of the peak value of the current wave. The tail value, $t_h = 50\ \mu s$, is defined as the time it takes until the wave drops till 50 percent of the peak value. System components can be exposed to very high lightning-induced overvoltages. The name plate of high-voltage equipment shows the *Lightning Impulse Withstand Voltage* (*LIWV*) adopted by IEC, or the *Basic Lightning Impulse Insulation Level* (*BIL*) adopted by IEEE, which is a standardized value for each voltage rating.

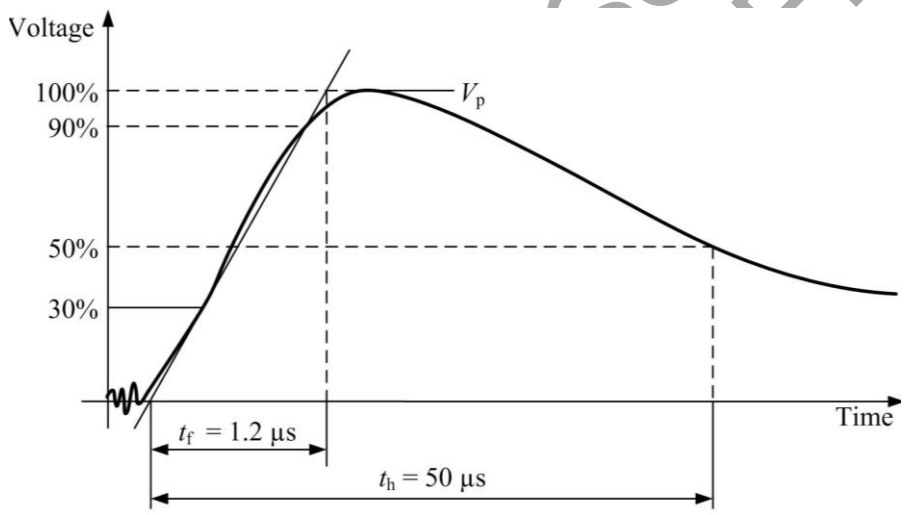

Figure 3. Standardized waveshape of a lightning-induced voltage wave.

The waveshape of Figure 3 can be described mathematically as the difference of two exponential functions:

$$e(t) = V_p(e^{-\alpha t} - e^{-\beta t}) \qquad (1)$$

In this expression, the parameter β is associated with the rise time t_f and the parameter α with the tail time t_h; that is the time measured during the tail at which the value of the waveshape reaches the 50% of the peak value (see Figure 3). With $\alpha = 1.4E4\ s^{-1}$ and $\beta = 4.5E6\ s^{-1}$, the double exponential expression of Eq. (1) results in a 1.2/50 μs waveshape.

Although the double exponential wave is easy to manipulate in mathematical analysis, the shape of actual lightning stroke currents is different. The usual double-exponential function to represent a transient waveshape has a discontinuity of its first derivative at $t = 0$, and it is not convenient for lightning calculations. Figure 4 shows the waveshape of the mean negative first stroke current as derived from Berger's work on Mount San Salvatore (Berger, Anderson, & Kroninger, 1975; Anderson & Eriksson, 1980). This waveshape has a concave wavefront with the greatest rate of change near the peak, and has been adopted by CIGRE.

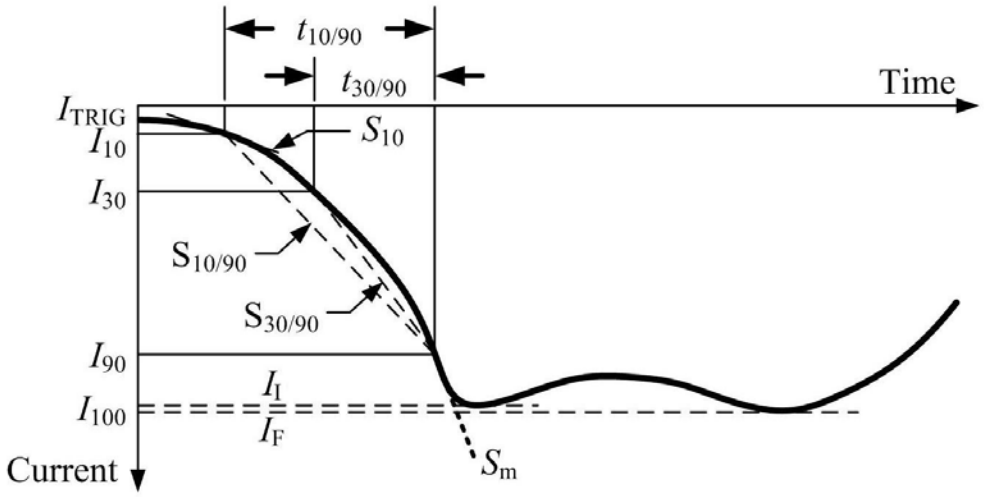

Parameter	Description
I_{10}	10% intercept along the stroke current waveshape
I_{30}	30% intercept along the stroke current waveshape
I_{90}	90% intercept along the stroke current waveshape
$I_{100} = I_I$	Initial peak of current
I_F	Final peak of current
$t_{10/90}$	Time between I_{10} and I_{90} intercepts on the wavefront
$t_{30/90}$	Time between I_{30} and I_{90} intercepts on the wavefront
S_{10}	Instantaneous rate-of-rise of current at I_{10}
$S_{10/90}$	Average steepness (through I_{10} and I_{90} intercepts)
$S_{30/90}$	Average steepness (through I_{30} and I_{90} intercepts)
S_m	Maximum rate-of-rise of current along wavefront, typically at I_{90}
$t_{d\ 10/90}$	Equivalent linear wavefront duration derived from $I_F/S_{10/90}$
$t_{d\ 30/90}$	Equivalent linear wavefront duration derived from $I_F/S_{30/90}$
t_m	Equivalent linear waveshape duration derived from I_F/S_m

Figure 4. Waveshape of typical negative return-stroke current.

Note that the current wave has two peaks, the second one being higher in magnitude. The front time is based on the first peak, and the peak amplitude on the second peak. The negative subsequent stroke current has, in general, shorter wave front than that of the negative first stroke current.

The negative subsequent stroke currents do not exhibit the pronounced concavity of the wavefront of the first stroke current. This is shown in Figure 5 (Anderson & Eriksson, 1980; IEEE TF, 2005). The concavity of the negative first stroke current (i.e., the initial slow rise followed by fast rise) may be attributed to the upward streamer from the object to be struck reaching out to the downward streamer from the cloud. The slow-rising upward streamer carries comparatively small current. However, when the upward streamer meets the downward leader, the current rises fast. As the subsequent strokes are not preceded by upward streamers, the wavefront of these strokes do not show the concavity.

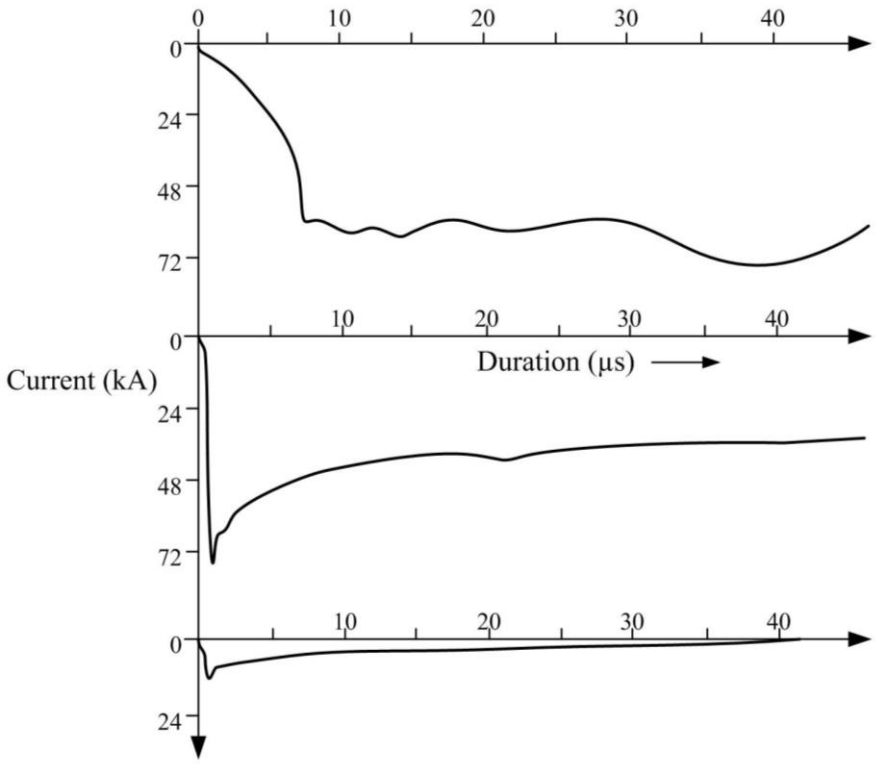

Figure 5. Examples of negative-polarity return-stroke currents. Uppermost curve: first stroke; middle curve: second stroke; bottom curve: third stroke.

Several empirical equations have been proposed for the waveshape of the negative first stroke current (CIGRE WG 33.01). A widely waveshape used to represent a lightning stroke current, with a concave waveshape and no discontinuity at $t = 0$, is the so-called Heidler's model (see Figure 6), which is given by (Heidler, Cvetic, & Stanic, 1999):

$$i(t) = \frac{I_{\mathrm{p}}}{\eta} \frac{k^n}{1+k^n} e^{-t/\tau_2} \tag{2}$$

where I_p $(=I_{100})$ is the peak current, η is a correction factor of the peak current, n is the current steepness factor, $k = t/\tau_1$, and τ_1, τ_2 are time constants determining current rise and decay time, respectively. The meaning of the parameters shown in Figure 6 is the same that for the waveshapes shown in Figures 3 and 4.

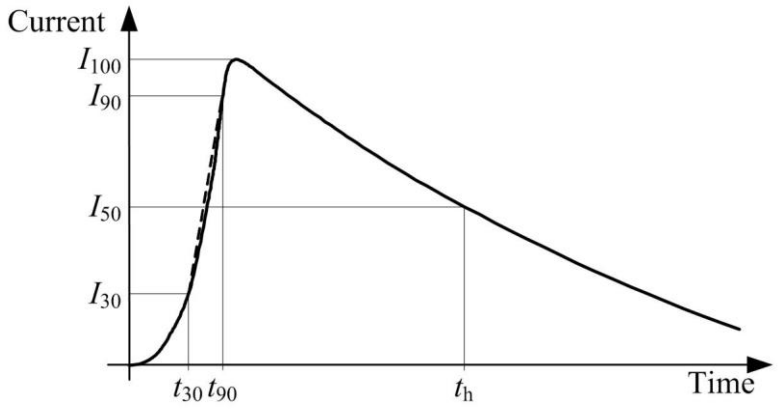

Figure 6. Heidler's waveshape for a lightning stroke current.

The waveshape of positive strokes exhibit larger peak currents, slower steepness, and longer mean time to crest and tail time than negative strokes. However, these conclusions have been derived from a limited number of field measurements and there are not enough common features to produce an acceptable positive-polarity mean waveshape (CIGRE WG 33.01, 1991; IEEE TF, 2005).

3.3. Lightning Parameters

A typical lightning stroke current may be characterized by a steep front rise, a broad peak area with several minor peaks and a slow decay to a low current, see Figure 4. For the calculation of lightning overvoltages, the critical part of the curve is the initial rise and the various parameters that are used to define the front and the crest. For the selection of surge arresters, the wave tail is also of concern.

Actual parameters are spread randomly and their probability distribution is described mathematically as a "log-normal" function. For instance, the probability density function of the return stroke peak current value I_p can then be expressed as (IEEE TF, 2005):

$$P(I_p) = \frac{1}{\sqrt{2\pi} I_p \sigma_{\ln I_p}} \exp\left[-\frac{z^2}{2}\right] \tag{3}$$

where

$$z = \frac{\ln I_{\mathrm{p}} - \ln I_{\mathrm{pm}}}{\sigma_{\ln I_{\mathrm{p}}}} \tag{4}$$

$\sigma_{\ln I_{\mathrm{p}}}$ is the standard deviation of I_{p}, and I_{pm} is the median value of I_{p}.

Tables 2 and 3 provide typical values of these parameters derived from field accumulated over the years. The tables show parameters summarized for both negative and positive flashes (Hileman, 1999; IEEE TF, 2005; Rakov & Uman, 2006; de la Rosa, 2007). These are the types of lightning flashes known to hit flat terrain and structures of moderate height. These data are amply used as primary reference in the literature on both lightning protection and lightning research.

Parameters	Units	First stroke		Subsequent strokes	
		Median	Log standard deviation	Median	Log standard deviation
Peak current (minimum 2 kA)	kA				
Initial I_{I}		27.7	0.461	11.8	0.530
Final I_{F}		31.1	0.484	12.3	0.530
Front duration	μs				
$t_{10/90}$		5.63	0.576	0.75	0.921
$t_{30/90}$		3.83	0.553	0.67	1.013
Steepness	kA/μs				
S_{10}		2.6	0.921	18.9	1.404
$S_{10/90}$		5.0	0.645	15.4	0.944
$S_{30/90}$		7.2	0.622	20.1	0.967
S_{m}		24.3	0.599	39.9	0.852
Stroke duration (2 kA to half peak value on the tail)	μs	77.5	0.577	30.2	0.933
Charge (total charge)	C	4.65	0.882	0.938	0.882
Action integral ($\int i^2 dt$)	$\mathrm{kA}^2\mathrm{s}$	0.057	1.373	0.0055	1.366
Time interval between strokes	ms	1st to 2nd stroke: Median = 45; σ = 1.066 2nd stroke onward: Median = 35 Log standard deviation for both = 1.066			

Table 2. Statistical parameters of negative flashes

Parameters	Units	Median	Log standard deviation
Peak current (minimum 2 kA) I_{p}	kA	35	1.21
Charge (total charge)	C	80	0.90
Front duration (from 2 kA to first peak)	μs	22	1.23

t_f			
Maximum di/dt S_m	kA/μs	2.4	1.54
Stroke duration (2 kA to half peak value on the tail) t_h	μs	230	1.33
Action integral ($\int i^2 dt$)	A^2s	6.5×10^5	1.91

Table 3. Statistical parameters of positive flashes

Peak current: Based on observation from various regions of the world, the frequency distribution of peak current magnitude for the first stroke of negative downward flashes to structures less than 60 m in height can be approximated by a log-normal function with a median of 31.1 kA and a standard deviation of the $\ln I_p$ of 0.484 kA. However, CIGRE recommends using an approximation based on two straight lines with the following parameters:

$$I_p < 20 \text{ kA} \qquad I_{pm} = 61.0 \text{ kA} \qquad \sigma_{\ln I_p} = 1.330 \text{ kA} \tag{5a}$$

$$I_p > 20 \text{ kA} \qquad I_{pm} = 33.3 \text{ kA} \qquad \sigma_{\ln I_p} = 0.605 \text{ kA} \tag{5b}$$

In general, no correlation can be established between first- and subsequent-stroke peak magnitudes, although it is accepted that the peak current of subsequent strokes is lower, reaching on average a peak which is a 40% of the first stroke peak. However, about 12% of subsequent strokes have larger peak current magnitude than the first stroke (CIGRE WG 33.01). Observed downward negative multi-stroke flashes show peak currents below 80 kA, with a frequency distribution that can be approximated by a log-normal function with a median of 12.3 kA and a standard deviation of $\ln I_p$ of 0.53 kA.

Typically, less than 10% of lightning flashes are of positive polarity, but the limited number of measurements does not permit a clear separation between downward and upward flashes. However, the proportion of positive to negative flashes is higher in autumn/winter. In general, positive flashes exhibit a greater peak current magnitude than negative downward flashes.

For a wide range of peak current values, the following expression can be used to obtain the cumulative probability of the first-stroke current peak value (Anderson, 1982):

$$P(I_p \geq I_0) = \frac{1}{1 + \left(\frac{I_0}{31}\right)^{2.6}} \tag{6}$$

where $P(I_p \geq I_0)$ is the probability that the first return stroke has a peak current I_p that exceeds I_0, the prospective first return stroke peak current (kA).

This expression has been adopted by IEEE WG (1985). This distribution is very close to the two-slope CIGRE distribution for the first stroke of negative downward flashes, except for the extremes, as shown in Figure 7, in which the two approaches are compared.

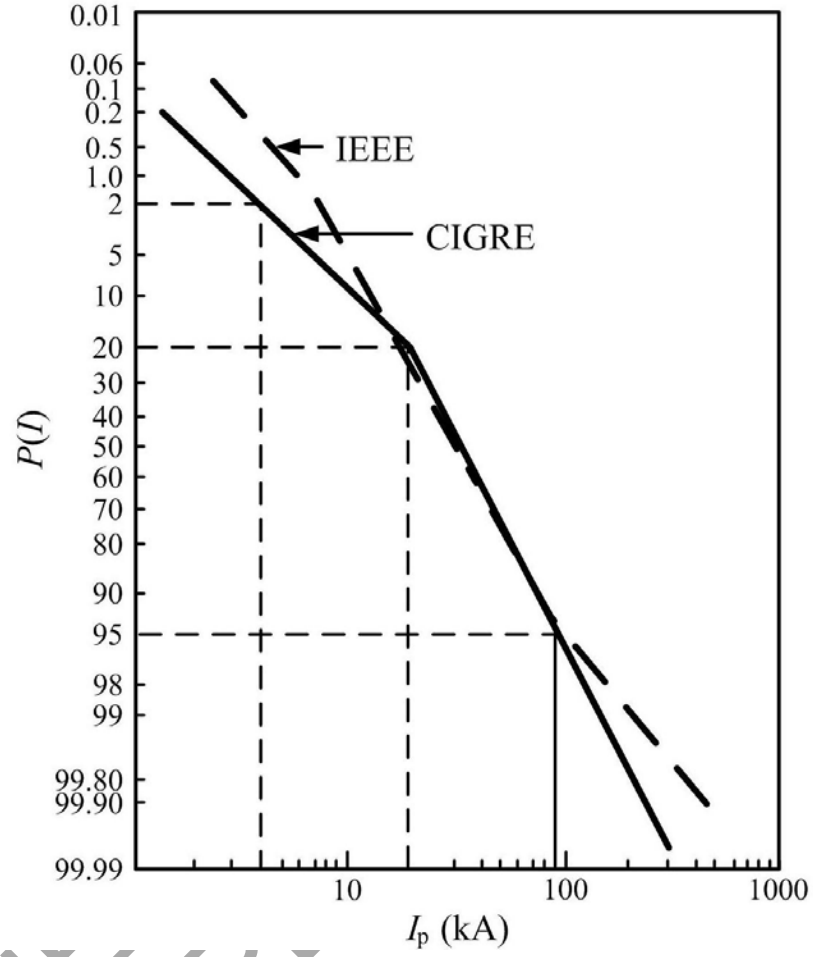

Figure 7. IEEE and CIGRE probability distributions of the first stroke of negative downward flashes.

The cumulative probability that a subsequent-stroke current will exceed a given level can be also estimated in a similar manner. The following simplified equation has been proposed (IEEE Std. 1243, 1997):

$$P(I_p \geq I_0) = \frac{1}{1+\left(\frac{I_0}{12}\right)^{2.7}} \tag{7}$$

where $P(I_p \geq I_0)$ is now the probability that the subsequent return stroke has a peak current I_p that exceeds I_0, the prospective subsequent return stroke peak current (kA).

Time-to-peak: Front-times of subsequent negative strokes are generally much shorter than those of the first stroke, and exhibit smaller disparity between front-duration

distributions due to their reduce concavity. For practical calculations, CIGRE recommends using the parameter t_{d30} $(= t_{30/90} / 0.6)$ for both first and subsequent strokes (CIGRE WG 33.01).

Steepness: High values of steepness occur for only short durations of wavefront, which justify the large difference in average and maximum steepness parameters. The steepness parameters of subsequent strokes are significantly higher and imply a significantly less pronounced degree of wavefront concavity than those of the first stroke.

Stroke duration: It can be defined as the time interval between 2 kA on the wavefront and the point of the wavetail where the current magnitude has fallen to 50% of the peak value.

Action integral: It is the energy that would be dissipated in a 1-Ω resistor if the lightning current was to flow through it (de la Rosa, 2007). This parameter can provide some insight on the understanding of damage to power equipment, including surge arresters, in power line installations.

3.4. Correlation Between Lightning Parameters

Table 4 is based on the conclusions summarized by de la Rosa (2007) and presents important findings for positive flashes, negative first strokes, and negative subsequent strokes. Table entries that are not filled in were not analyzed by any author.

Lightning Parameter	Correlation (Correlation Coefficient)
Positive Flashes	
Front time (t_f)	Low (0.18)
Peak rate-of-rise (dI/dt)	Moderate (0.55)
Impulse charge (Q_{imp})	High (0.77)
Flash charge (Q_{flash})	Moderate (0.59)
Flash action integral (W_{flash})	High (0.76)
Negative First Strokes	
Front time (t_f)	Low (—)
Peak rate-of-rise (dI/dt)	Moderate/high (—)
Impulse charge (Q_{imp})	High (0.75)
Flash charge (Q_{flash})	Low (0.29)
Impulse action integral (W_{imp})	High (0.86)
Negative Subsequent Strokes	
Front time (t_f)	Low (0.13)
Peak rate-of-rise (dI/dt)	High (0.7–0.8)

Table 4. Correlation between lightning parameters

A moderate-to-high correlation is found between lightning current and all but peak rate of rise in positive flashes. Therefore, extreme heating should be expected in arcing or transient currents conducted through protective devices following insulation flashover produced by positive lightning flashes. Note that lightning parameters associated with heat are charge and action integral and that rate-of-change of lightning current is connected with inductive effects. Heating effects, however, are loosely correlated with peak current, since correlation coefficient for the total charge (Q_{flash}) is poor.

3.5. Ground Flash Density and Keraunic Level

Ground flash density, also referred to as GFD or N_{g}, is a long-term average value defined as the number of lightning flashes striking ground per unit area and per year. The GFD level is an important parameter to consider for the design of electric power facilities. This is due to the fact that power line performance and damage to power equipment are considerably affected by lightning.

Where GFD data from lightning location systems is not available, GFD can be determined as a function of the *keraunic level*, which is a rather coarse measurement in the form of counters depicting number of days (24 hour period) per year on which thunder is heard. The keraunic-level data is usually available for a number of years all over the world as a function of T_{D} (thunder days or keraunic level) or T_{H} (thunder-hours) (IEEE Std 1410, 2010). Basically, any of these parameters can be used to get a *rough* approximation of GFD by using the following expressions:

$$N_{\text{g}} = 0.040 T_{\text{D}}^{1.25} \quad \text{flashes/km}^2\text{/year} \tag{8a}$$

$$N_{\text{g}} = 0.054 T_{\text{H}}^{1.10} \quad \text{flashes/km}^2\text{/year} \tag{8b}$$

A low incidence of lightning does not necessarily mean an absence of lightning-related problems. Power lines, for example, are prone to failures even if the ground flash density levels are low when they span across hills or mountains, where achieving a low tower footing impedance becomes difficult (de la Rosa, 2007).

4. Incidence of Lightning to Overhead Lines

4.1. Introduction

The first step in the study of the lightning performance of an overhead power line is to estimate the number of lightning surges to the line. Lightning overvoltages in overhead lines may be caused by a direct stroke to a line or by a stroke that impact to ground in the vicinity of the line. The impact of strokes will give rise to overvoltages which may exceed the insulation level provided by insulators or may cause flashover between conductors or between conductors and the tower structure.

The effect of direct strokes is important for protection of overhead lines. A direct stroke to a shielded line may impact to a phase conductor (*shielding failure*) or to a shield

wire. In this case, the impact may be to a tower or to a midpoint of the shield wire; the overvoltage caused in any of these two scenarios may cause the so called *backflashover*. The application of a model that can estimate the number of strokes to phase conductors or to shield wires is useful for the design of the line shielding.

Indirect strokes may induce voltage that are of concern only for distribution lines. Nearby lightning strokes to ground induce overvoltages that very rarely will exceed 200 kV; this will not threat the insulation strength of transmission lines but may exceed the insulation strength of many distribution lines.

4.2. The Electrogeometric Model

As the downward leader approaches the ground, a point of discrimination is reached for a final leader step. The model for the final jump is based on the specific value of the stroke current (Hileman, 1999): (i) given the stroke current, the velocity is estimated; (ii) the potential of the downward leader is derived from the velocity; (iii) the striking distance is found as the relationship between potential and breakdown gradient of the downward leader. Local electric field gradients around conductors are somewhat higher than at ground level, and the striking distance of a conductor r_c is usually considered to be greater than the striking distance to ground r_g.

Figure 8 illustrates the application for a two-conductor geometry. Arcs of circles with the radii r_c are drawn centered at both conductors; the phase conductor and the shield wire. A horizontal line is then drawn at a height r_g from ground. If a downward leader, having a prospective current I_p for which the arcs were drawn, touches the arcs between A and B, the leader will strike the phase conductor. If the leader touches between B and C, it will strike the shield wire. If all leaders are considered vertical, the exposure distance for a shielding failure is D_c. In the case shown in Figure 8, the stroke will proceed directly to the ground, without hitting any conductor if the vertical downward leader is at the right of A.

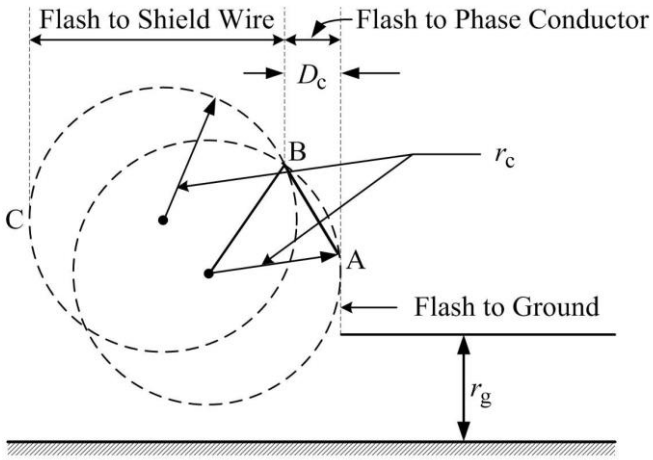

Figure 8. Exposed distance for final jump in electrogeometric model.

A number of formulas for calculating the striking distances have been developed by various authors. The general form for most expressions is (Hileman, 1999; Chowdhuri, 1996; IEEE Std. 1243, 1997; IEEE Std 1410, 2010):

$$r_s = AI_p^b \tag{9}$$

where I_p is the return stroke current.

Table 5 shows the most common expressions and the authors or international committees who proposed those expressions.

Author	Striking Distance to Phase Conductors and Ground Wires (meters)	Striking Distance to Ground (meters)
Wagner (1961)	$r_c = 14.2I_p^{0.42}$	$r_g = 14.2I_p^{0.42}$
Young (1963)	$r_c = 27.0I_p^{0.32}$ para $h < 18$ m $r_c = \frac{444}{462-h}27.0I_p^{0.32}$ para $h > 18$ m	$r_g = 27.0I_p^{0.32}$
Brown & Whitehead (1969)	$r_c = 7.1I_p^{0.75}$	$r_g = 6.4I_p^{0.75}$
Eriksson (1982)	$r_c = 0.67h^{0.6}I_p^{0.74}$	None
IEEE WG (1985)	$r_c = 8I_p^{0.65}$	$r_g = \beta 8I_p^{0.65}$ $\begin{cases}\beta = 0.64 & \text{for UHV lines}\\ \beta = 0.80 & \text{for EHV lines}\\ \beta = 1.0 & \text{for others}\end{cases}$
IEEE Std 1243 (1997)	$r_c = 10I_p^{0.65}$	$r_g = [3.6 + 1.7\ln(43-h)]I_p^{0.65}$ $h < 40$ m $r_g = 5.5I_p^{0.65}$ $h \geq 40$ m

Table 5. Expressions for the striking distances

An important approach for estimating the lightning incidence to overhead power lines is that proposed by Eriksson. According to this model, the striking distances are given for the phase conductor and the overhead shield wire, but there is no striking distance to ground (Eriksson, 1987a). Figure 9 shows the attractive radius derived from this model. Construct a horizontal line at the height of the of the wire and an arc of radius r_a with a center at the wire; downward leaders with a vertical channel between A and B will terminate on the wire, otherwise they will proceed to ground.

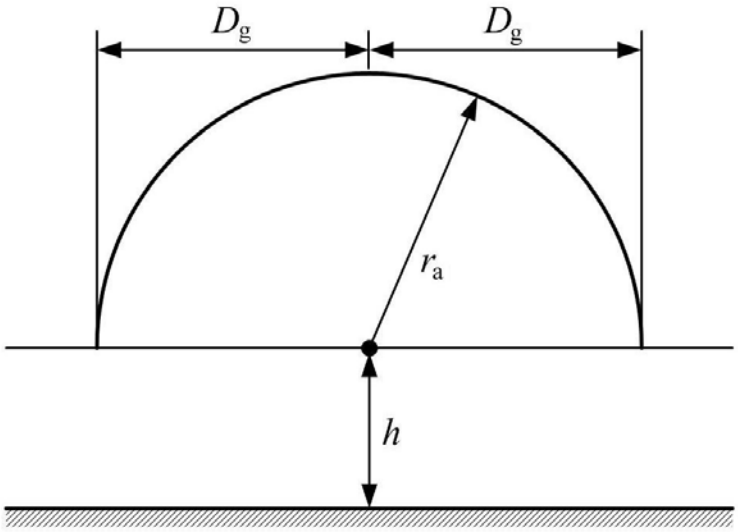

Figure 9. Incidence of lightning strokes based upon Eriksson's geometric model.

For heights from 10 to 100 meters, Eriksson derived the following expression for the so-called attractive radius:

$$r_a = 0.84h^{0.6}I_p^{0.74} \tag{10}$$

where h is in meters, I_p is in kA, and r_a is in meters.

He also suggested another relation for the attractive radius, independent of the stroke current and solely dependent upon the height of the object (Eriksson, 1987a; Eriksson, 1987b):

$$r_a = 14h^{0.6} \tag{11}$$

4.3. Application of the Electrogeometric Model

The procedure for applying the electrogeometric model for a single wire (see Figure 10a) is that presented above: (i) calculate the striking distances r_c and r_g for a specific stroke current I_p; (ii) draw a parallel phase-to-ground at height r_g and an arc of radius r_c with centre at the wire. Any stroke with a vertical leader between A and B will terminate on the wire, and any stroke to the left of A or the right of B will terminate to ground.

The number of strokes with a given current I_p terminating on the wire is:

$$N(G)\big|_{I_p} = 2N_g D_g \ell \tag{12}$$

where N_g is the ground flash density, D_g is the exposed section, and ℓ is the line length. Remember that N_g is usually given in flashes per square kilometer per year.

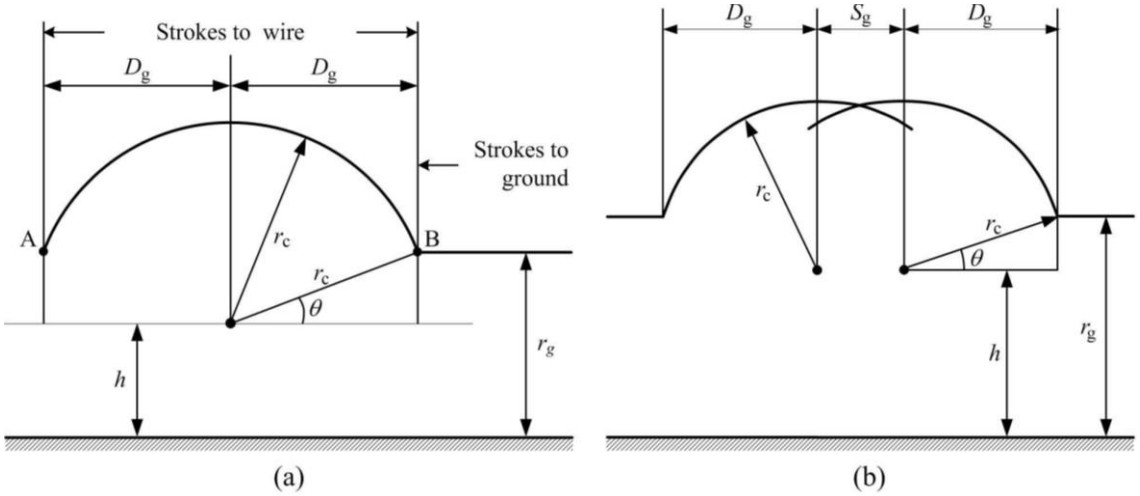

Figure 10. Incidence of lightning strokes based upon the electrogeometric model. (a) One wire. (b) Two wires.

If the probability of this current is $f(I_p)dI_p$, the total number of strokes of current I_p is:

$$dN(G) = 2N_g D_g \ell f(I_p) dI_p \tag{13}$$

and total number of strokes that will terminate on the wire is:

$$N(G) = 2N_g \ell \int_3^\infty D_g f(I_p) dI_p \tag{14}$$

Note that a recommended lower integration limit of 3 kA has been used, which assumes that there cannot be a stroke with zero current and there is a lower limit for the stroke current (CIGRE WG 33.01, 1991).

For a case with two wires separated a distance S_g, the geometric construction is shown in Figure 10b. Following a similar procedure, the number of strokes that will terminate on a wire is calculated as:

$$N(G) = 2N_g \ell \int_3^\infty D_g f(I_p) dI_p + N_g \ell S_g \tag{15}$$

The number of strokes to any of the geometries shown in Figure 11 can be easily calculated by means of the Eriksson's model. The area exposed to lightning is given by:

$$A_e = (2r_a + S_g)\ell \tag{16}$$

in which the attractive radius r_a is obtained from Eq. (11). In this expression S_g is zero for single wire geometry, see Figure 11.

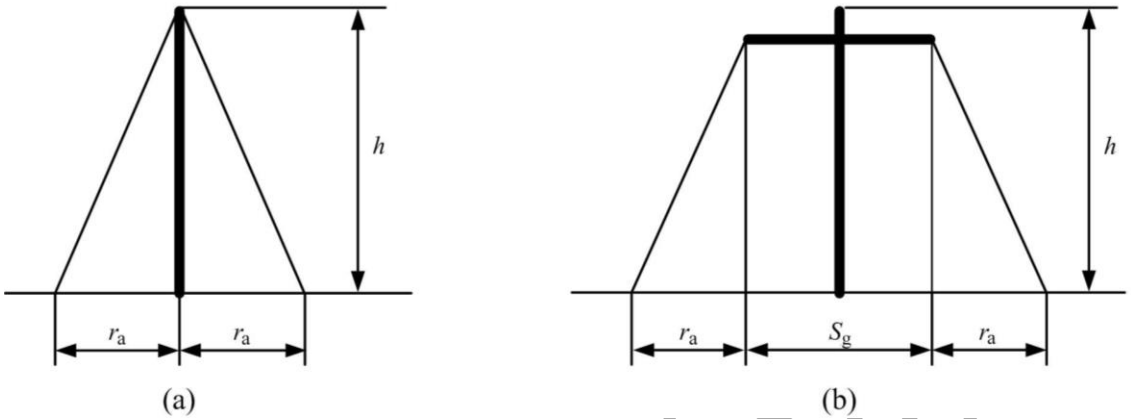

Figure 11. Incidence of lightning strokes based upon the attractive radius – Eriksson's model.

The number of flashes striking the line per 100 km and per year is then obtained from (Eriksson, 1987b):

$$N = N_g\left(\frac{28h^{0.6} + S_g}{10}\right) \tag{17}$$

An important aspect when analyzing the lightning exposure of overhead power lines is that they can be shielded by nearby objects (e.g., building, trees) along their corridors; that is, tall objects in the vicinity of the line may divert lightning flashes. This will decrease the number of direct strokes estimated by Eq. (17) to a degree determined by the distance and height of the objects. This shielding may have a significant effect on distribution lines, but it is not usually considered for transmission lines.

-
-
-

Bibliography

Agrawal A.K., Price H.J., Gurbaxani S.H. (1980). Transient response of a multiconductor transmission line excited by a non-uniform electromagnetic field, *IEEE Trans. on Electromagnetic Compatibility* **22**,

119-129. [This paper presents two formulations of the time-domain transmission-line equations for uniform multiconductor transmission lines in a conductive, homogeneous medium excited by a transient, non-uniform electromagnetic (EM) field].

Anderson J.G. (1982). Lightning Performance of Transmission Lines. Chapter 12 of *Transmission Line Reference Book, 345 kV and Above*, 2nd Edition, EPRI, Palo Alto, CA. [This chapter reviews the main factors that affect the lightning performance of an overhead transmission line (lightning parameters, line design), proposes a simplified modeling approach of a transmission line for lightning overvoltage calculations, and presents a step-by-step, linearized numerical solution for estimating the lightning performance of overhead transmission lines].

Anderson R.B., Eriksson A.J. (1980). Lightning parameters for engineering application, *Electra* **69**, 65-102. [This report presents updated information about the parameters of the lightning ground flash required for engineering applications. The parameters discussed in the report are related to lightning incidence, peak current amplitude, and impulse shape].

Baldo G., Hutzler B., Pigini A., Garbagnati E. (1992). Dielectric strength under fast front overvoltages in reference ambient conditions, Chapter 5 of CIGRE WG 33.01, Guide for the Evaluation of the Dielectric Strength of External Insulation, CIGRE Technical Brochure no. 72. [This chapter discusses the different factors that affect the lightning strength of the most common insulation configurations and provides approaches for evaluating this strength under both standard and non-standard lightning impulses].

Berger K., Anderson R.B., Kroninger H. (1975). Parameters of lightning flashes, *Electra* **41**, 23-37. [This paper defines the parameters to be used for lightning characterization and provides the representative lightning current shapes and parameters derived from field measurements carried out during the period from 1963 to 1971].

Borghetti A., Nucci C.A., Paolone M. (2007). An improved procedure for the assessment of overhead line indirect lightning performance and its comparison with the IEEE Std. 1410 method, *IEEE Trans. on Power Delivery* 22, 684-692. [This paper presents a procedure for the estimation of the annual number of lightning-induced flashovers versus the critical flashover voltage of the line insulators. The paper includes a comparison between the new procedure is compared and that described in IEEE Std. 1410-2004, and a discussion of the differences in the results predicted by the two methods].

Brown G.W., Whitehead E.R. (1969). Field and analytical studies of transmission line shielding: Part II, *IEEE Trans. on Power Apparatus and Systems* 88, 617-626. [This paper proposes and extension of the model for the shielding of transmission lines against lightning to the case of partially effective shielding, including the effect of possible leader approach angle distributions, and develops an index number to aid in classifying line performance].

Chowdhuri P. (2003). *Electromagnetic Transients in Power Systems*, 2nd Edition, Taunton, UK: RS Press-John Wiley. [This book presents the basic theories of the generation and propagation of electromagnetic transients in power systems, discusses the performance of power apparatus under transient voltages and introduce the principles of protection against overvoltages].

CIGRE WG 01.33 (1991). Guide to Procedures for Estimating the Lightning Performance of Transmission Lines, CIGRE Brochure no. 63. [This brochure presents a detailed description of models and procedures for estimating the outage rate of transmission lines due to lightning].

CIGRE WG 33.01 (Lightning) (1995). Lightning-induced voltages on overhead power lines, Part I: Return-stroke current models with specified channel-base current for the evaluation of the return-stroke electromagnetic fields, *Electra* 161, 75-102. [This first part of the report is aimed at presenting the models to be considered for representing return stroke currents (as a function of height and time) needed for the calculation of induced electromagnetic fields, and providing the equations for obtaining these fields].

CIGRE WG 33.01 (Lightning) (1995). Lightning-induced voltages on overhead power lines, Part II: Coupling models for the evaluation of the induced voltages, *Electra* 162, 121-145. [This second part of the report presents a comparison of different coupling models for calculation of lightning induced voltages and a discussion about the factors that may have some influence in the differences between theoretical calculations and field measurements].

CIGRE WG 33.02 (1990). Guidelines for Representation of Network Elements when Calculating

Transients, CIGRE Brochure no. 39. [This brochure presents a review of guidelines proposed for representing power system components when calculating electromagnetic transients by means a computer].

CIGRE WG C4.401 (2005). Lightning induced voltages on overhead power lines. Part III: Sensitivity analysis, *Electra* 222, 27-30. [This paper summarizes the main result of a sensitivity analysis aimed on the influence of the most important parameters which determine intensity and wave shape of lightning-induced voltages].

Cooray V. (2002). Some consideration on the 'Cooray-Rubinstein' approximation used in deriving the horizontal electric field over finitely conducting ground, *IEEE Trans. on Electromagnetic Compatibility*, 44 560-566. [This paper studies the accuracy with which the "Cooray-Rubinstein" formulation can predict the horizontal electric field generated by lightning return strokes, and provides a simple modification that improves the accuracy to better than about 5%].

Darveniza M. (2007). A practical extension of Rusck's formula for maximum lightning induced voltage that accounts for ground resistivity, *IEEE Trans. on Power Delivery* **22**, 605-612. [This paper reviews the effects of ground resistivity on overhead line voltages induced by nearby lightning flashes to ground, describes data from both experimental field measurements and analytical studies of these effects, and proposes a semi-empirical extension to Rusck's formula for maximum induced voltage to account for the effect of ground resistivity].

Das J.C. (2010). *Transients in Electrical Systems. Analysis, Recognition, and Mitigation*, New York, NY: McGraw-Hill. [A practical and analytical guide for practicing engineers, and a reference book on transients in power systems].

de la Rosa F. (2007). Characteristics of Lightning Strokes, Chapter 6 of *Power Systems*, L.L. Grigsby (ed.), Boca Raton, FL: CRC Press. [This chapter discusses the lightning parameters that are important for the assessment of lightning performance of power transmission and distribution lines].

Dommel H.W., (1992). *EMTP Theory Book*, 2nd Edition, Vancouver, BC, Canada: Microtran Power System Analysis Corporation. [This book is the reference text book for the Electromagnetic Transients Program].

Elahi H., Sublich M., Anderson M.E., Nelson B.D. (1990). Lightning overvoltage protection of the Paddock 362-145 kV gas insulated substation, *IEEE Trans. on Power Delivery* **5**, 144-149. [This paper presents an EMTP analysis of backflashovers close to the Paddock 362-145 kV gas-insulated substation using a frequency-dependent multiconductor system. The analysis is aimed at better evaluation of lighting protection requirements for GIS protected by metal-oxide surge arresters].

Eriksson A.J. (1987a). The incidence of lightning strikes to power lines, *IEEE Trans. on Power Delivery* **2**, 859-870. [This paper addresses the lightning attractive radius concept and procedures for estimating the number of lightning flashes to power lines. A generalized expression for estimating strike incidence is presented].

Eriksson A.J. (1987b). An improved electrogeometric model for transmission line shielding analysis, *IEEE Trans. on Power Delivery* 2, 871-886. [This paper presents a new electrogeometric model intended for transmission line lightning shielding analysis and based upon previous empirical and analytical studies of the lightning striking process. The model is essentially independent of any assumptions regarding striking distances to ground].

Gallagher T.J., Dudurych I.M. (2004). Model of corona for an EMTP study of surge propagation along HV transmission lines, *IEE Proc.-Gener. Transm. Distrib.* 151, 61-66. [This paper proposes a mathematical model of the phenomenon of corona on an HV transmission line for implementation in EMTP as a user-defined component]. The new model is verified thoroughly by an extensive comparison of the simulation results with both direct measurements and results of simulations by other authors].

Gole A.M., Martinez-Velasco J.A., Keri A.J.F. (Eds.) (1999). Modeling and Analysis of System Transients Using Digital Programs, *IEEE PES Special Publication*, TP-133-0. [This special publication presents an introduction to time-domain solution of electromagnetic transients in power systems using a digital computer. The publication covers two main topics: solution techniques and modeling of power components].

Greenwood A. (1991). *Electrical Transients in Power Systems*, New York. NY: John Wiley. [A reference book for the analysis of transient processes in electrical power systems].

Heidler F., Cvetic J.M., Stanic B.V. (1999). Calculation of lightning current parameters, *IEEE Trans. on Power Delivery* 14, 399-404. [This paper proposes an algorithm for a fast calculation of the channel-base current parameters. This algorithm can be used for both lightning current modeling in power engineering and the research of the radiated lightning electromagnetic pulse and its coupling with overhead lines and other metallic structures.]

Hileman A.R. (1999). *Insulation Coordination for Power Systems*, New York, NY: Marcel Dekker. [A detailed and comprehensive reference book for power system insulation coordination].

IEC 60071-1 (2010). Insulation co-ordination - Part 1: Definitions, principles and rules. [First part of the IEC standard on Insulation Co-ordination in which the procedure for the selection of the rated withstand voltages for the phase-to-earth, phase-to-phase and longitudinal insulation of the equipment and the installations with voltage above 1 kV is specified. The document gives also the lists of the standard withstand voltages from which the rated withstand voltages should be selected].

IEC 60071-2 (1996). Insulation co-ordination, Part 2: Application guide. [Second part of the IEC standard on Insulation Co-ordination in which the application guide of the procedure presented in the fist part is detailed. The standard provides guidance for the determination of the rated withstand voltages and justifies the association of these rated values with the standardized highest voltages for equipment].

IEC 60071-4 (2004). Insulation co-ordination - Part 4: Computational guide to insulation co-ordination and modelling of electrical networks. [A technical report aimed at providing guidelines in terms of methods and models adapted to the use of numerical programmes for conducting insulation co-ordination studies based of the approaches presented in IEC standard 60071].

IEEE Std 1243 (1997). IEEE Guide for improving the lightning performance of transmission lines. [A guide aimed at providing criteria for improving the lightning performance of transmission lines. The standard discusses the effect of routing, structure type, insulation, shielding, and grounding, and contains simple equations, tables, and graphs that can be useful to design an overhead power transmission line with minimum lightning interruptions].

IEEE Std 1313.1 (1996). IEEE Standard for Insulation Coordination – Definitions, Principles and Rules. [This standard define applicable terms to three-phase ac systems above 1 kV for insulation coordination purposes, identifies standard insulation levels, and specifies the procedure for selection of the withstand voltages for equipment insulation systems].

IEEE Std 1313.2 (1999). IEEE Guide for the Application of Insulation Coordination. [An application guide aimed at providing guidance in the determination of the withstand voltages and suggesting calculation methods and procedures. The guide is basically intended for air-insulated ac systems].

IEEE Std 1410 (2010). IEEE Guide for Improving the Lightning Performance of Electric Power Overhead Distribution Lines. [A guide written for the distribution-line designer. The standard identifies factors that contribute to lightning-caused faults on overhead distribution lines, contains information on methods to improve the lightning performance of overhead distribution lines, and suggests improvements to existing and new constructions].

IEEE TF on Fast Front Transients (A.F. Imece, chair) (1996). Modeling guidelines for fast front transients, *IEEE Trans. on Power Delivery* **11**, 493-506. [This paper provides modeling guidelines for application in digital simulations of fast front electromagnetic transients (i.e., frequency range from 10 kHz up to 1 MHz), with particular emphasis on lightning surge analysis of overhead power lines and substations].

IEEE TF on Parameters of Lightning Strokes (2005). Parameters of lightning strokes: A review," *IEEE Trans. on Power Delivery* **20**, 346-358. [This paper presents the statistical data of the significant parameters (peak current, waveshape and velocity of the return stroke, the total flash charge and $\int I^2 dt$) of lightning flash, collected by many researchers over many years around the world.

IEEE WG on Lightning Performance of Transmission Lines (1985). A simplified method for estimating lightning performance of transmission lines, *IEEE Trans. on Power Apparatus and Systems* **104**, 919-932. [This paper presents a simplified method for estimating the lightning performance of overhead transmission lines. The method, which incorporates newly available information on lightning

characteristics checked against existing line performance and is based on the work by Anderson (1982), has been coded as a computer program].

IEEE WG on Lightning Performance of Transmission Lines (1993). Estimating lightning performance of transmission lines II: Updates to analytical models, *IEEE Trans. on Power Delivery* **8**, 1254-1267. [This paper is an update of a previously paper by the same IEEE WG published in 1985].

Ishii M., Michishita K., Hongo Y., Oguma S. (1994). Lightning-induced voltage on an overhead wire dependent on ground conductivity, *IEEE Trans. on Power Delivery* **9**, 109-118. [This paper presents a solution of lightning-induced voltages on an overhead wire by means of the Telegrapher's equation, in combination with numerical calculations of electric fields from return stroke currents as inducing sources. The accuracy of the solution is tested by comparison with the experimental results obtained from a geometrical model on a finitely conducting ground].

Lee K.C. (1983). Non-linear corona models in the Electromagnetic Transients Program, *IEEE Trans. on Power Apparatus and Systems* **102**, 2936-2942. [This paper describes the EMTP implementation of a numerical model representing the non-linear corona phenomenon for lightning overvoltage studies using single phase representation of multi-phase transmission line for distances shorter than 2 km are used].

Martinez J.A., Castro-Aranda F. (2005). Lightning performance analysis of overhead transmission lines using the EMTP, *IEEE Trans. on Power Delivery* **20**, 2200-2210. [This paper presents a procedure, implemented in an EMTP-like tool, for the calculation of lightning flashover rates of transmission lines using a Monte Carlo method. Some refinements are proposed to decrease the computer time while preserving the accuracy of calculations].

Martinez-Velasco J.A., Ramirez A.I., Dávila M. (2009). Overhead Lines, Chapter 2 of *Power System Transients. Parameter Determination*, J.A. Martinez-Velasco (ed.), Boca Raton, FL: CRC Press. [This chapter details the different models that can be used for representing the various part of overhead transmission lines (conductors, shield wires, towers, insulators, footing impedances) in transient analysis and simulation, and presents procedures for determining the parameters to be specified in those models].

Mousa A.M. (1994). The soil ionization gradient associated with discharge of high currents into concentrated electrodes, *IEEE Trans. on Power Delivery* **9**, 1669-1677. [The grounding resistance of a concentrated electrode depends on the magnitude of the of the soil and drops when it is subjected to a high current charge. Based on both a theoretical analysis and a critical review of the large number of available measurements, this paper recommends that the soil ionization gradient be taken equal to 300 kV/m for typical soils].

Nucci C.A., Rachidi F., Ianoz M., Mazzetti C. (1993). Lightning induced voltages on overhead lines, *IEEE Trans. on Electromagnetic Compatibility* **35**, 75-86. Correction published in no. 4, p. 488, November 1993. [This paper presents a discussion on modeling procedures for calculation of lightning-induced voltages on overhead lines].

Paolone M., Nucci C.A., Petrache E., Rachidi F. (2004). Mitigation of lightning-induced overvoltages in medium voltage distribution lines by means of periodical grounding of shielding wires and of surge arresters: Modeling and experimental validation, *IEEE Trans. on Power Delivery* **19**, 423-431. [This paper investigates the effect of periodically-grounded shielding wires and surge arresters on the attenuation of lightning-induced voltages. The computation results are validated by comparison with calculations obtained by other authors and with experimental results obtained using a reduced-scale line model illuminated by a nuclear electromagnetic pulse (NEMP) simulator].

Pigini A,.Rizzi G., Garbagnati E., Porrino A., Baldo G., & Pesavento G. (1989). Performance of large air gaps under lightning overvoltages: Experimental study and analysis of accuracy of predetermination methods, *IEEE Trans. on Power Delivery* **4**, 1379-1392. [This paper summarizes the main findings of a research on the performance of large air gaps under impulses simulating lightning overvoltages, and proposes an improvement of existing models].

Rachidi F., Nucci C.A., Ianoz M., Mazzetti C. (1996). Influence of a lossy ground on lightning-induced voltages on overhead lines, *IEEE Trans. on Electromagnetic Compatibility* **38**, 250-264. [This paper presents a study on the effect of a lossy ground on the induced voltages on overhead power lines by a nearby lightning strike. The aim is to discuss and analyze the various simplified approaches and techniques proposed for the calculation of the fields and the line constants when the ground cannot be

assumed as a perfectly conducting plane. A comparison between several simplified expressions is presented and the validity limits of these expressions are established].

Rakov V.A., Uman M.A. (2006). *Lightning. Physics and Effects*, Cambridge UK: Cambridge University Press. [A reference book that covers all aspects related to lightning: physics, protection, and interaction with objects and systems].

Rakov V.A., Uman M.A., Fernandez M.I., Mata C.T., Rambo K.J., Stapleton M.V., Sutil R.R. (2002). Direct lightning strikes to the lightning protective system of a residential building: triggered-lightning experiments, *IEEE Trans. on Power Delivery* **17**, 575-586. [This paper describes the main characteristics of a test house connected to the secondary of a padmount distribution transformer. The test installation is aimed at analyzing the effects of direct lightning strikes to the lightning protective system. Lightning is triggered from natural thunderclouds using the rocket-and-wire technique. The paper includes a discussion of the main conclusions derived from field measurements].

Rubinstein M. (1996). An approximate formula for the calculation of the horizontal electric field from lightning at close, intermediate, and long range, *IEEE Trans. on Electromagnetic Compatibility* **38**, 531-535. [This paper presents an approximate formula to calculate the horizontal electric field from lightning. The formula is applicable for close, intermediate, and long distances to the lightning, at ground level and at a height above ground, can be used for numerical calculations in the frequency and in the time domains, and may be particularly useful for the calculation of lightning induced voltages].

Suliciu M.M., Suliciu I. (1981). A rate type constitutive equation for the description of the corona effect, *IEEE Trans. on Power Apparatus and Systems* **100**, 3681-3685. [This paper proposes a rate type model for the description of the corona effect. The model, which may be used to study wave attenuation due to corona discharges, includes the relaxation properties of an electric line due to the presence of this effect].

Young F.S., Clayton J.M., Hileman A.R. (1963). Shielding of transmission lines, *IEEE Trans. on Power Apparatus and Systems* **82**, 132-154. [This paper presents a method for determining striking distances based on a streamer type breakdown from the leader tip potential. The proposed method is a modification of the Wagner's model and results in two different striking distances to phase conductors and shield wires, depending on the transmission line tower height].

van der Sluis L. (2001). *Transients in Power Systems*, Chichester, UK: John Wiley. [An introduction to transients in power systems with a coverage of insulation co-ordination standards and a guidance in the testing of high-voltage circuit breakers].

Wagner C.F., Gross I.W., Lloyd B.L. (1954). High-voltage impulse test on transmission lines, *AIEE Trans.* **73**, 196-210. [The results of tests carried out with a full-scale outdoor laboratory for determining the loss and radio influence under corona conditions on extra-high-voltage lines are reported. This paper is concerned with the line characteristics].

Wagner C.F., Hileman A.R. (1961). The lightning stroke-II, *Trans. AIEE on Power Apparatus and Systems* **80**, 622-642. [This paper presents a new mechanism of the leader steps and a theoretical description of the very important events that occur during the early stages of the return stroke].

Wagner C.F., Hileman A.R. (1963). Effect of pre-discharge currents on line performance, *IEEE Trans. on Power Apparatus and Systems* **82**, 117-131. [Pre-discharge currents of gaps under impulse conditions produce drops at 2 or 3 microseconds that may be equal to or greater than the gap voltage. This paper presents the determination of the magnitude of theses currents and suggests that the adaptation of their properties improves the lightning performance of transmission lines].

Biographical Sketches

Juan A. Martinez-Velasco was born in Barcelona (Spain). He received the Ingeniero Industrial and Doctor Ingeniero Industrial degrees from the Universitat Politècnica de Catalunya (UPC), Spain. He is currently with the Departament d'Enginyeria Elèctrica of the UPC. His teaching and research areas cover Power Systems Analysis, Transmission and Distribution, Power Quality and Electromagnetic Transients. He is an active member of several IEEE and CIGRE Working Groups. Presently, he is the chair of the IEEE WG on Modeling and Analysis of System Transients Using Digital Programs.

Ferley Castro-Aranda was born in Tulua (Colombia). He received the Electrical Engineer degree from Universidad del Valle (Cali, Colombia) in 1992 and the Ph.D. degree in Electrical Engineering from Universitat Politècnica de Catalunya (Barcelona, Spain) in 2005. He is an Associate Professor at Universidad del Valle. His research interests are focused on Power Quality, High Voltage Test Equipment, Insulation Coordination and System Modeling for Transient Analysis using EMTP. Currently, he is the Manager of the High Voltage Laboratory at Universidad del Valle.